Future Energy
Open Access Journal
ISSN 2832-0328

May 2026| Volume 05 | Issue 02 | Pages 01-11

Journal homepage: https://fupubco.com/fuen

https://doi.org/10.55670/fpll.fuen.5.2.1

Future Publishing LLC

Article

Experimental investigation of MHD mixed convection in an inclined elliptic enclosure saturated with Al_2O_3-water nanofluid

T. Adekeye[1]*, P.O. Okekunle[2], I. K. Adegun[3]

[1]Department of Mechanical Engineering, Faculty of Engineering and Technology, Kwara State University, Malete, Kwara State, Nigeria
[2]Department of Mechanical Engineering, Faculty of Engineering and Technology, Ladoke Akintola University of Technology, Ogbomoso, Oyo State, Nigeria
[3]Department of Mechanical Engineering, Faculty of Engineering and Technology, University of Ilorin, Ilorin, Kwara State, Nigeria

ARTICLE INFO

Article history:
Received 25 September 2025
Received in revised form
15 November 2025
Accepted 20 January 2025

Keywords:
Experimental investigation,
MHD mixed convection, Inclination effect,
Heat transfer, Laminar flow, Nanoparticle

*Corresponding author
Email address:
tundeadekeye2008@gmail.com

DOI: 10.55670/fpll.fuen.5.2.1

ABSTRACT

This study experimentally investigated the effects of geometric parameters, inclination, magnetohydrodynamic properties, flow-on-flow behaviour, and axial heat transfer in an oriented elliptic enclosure filled with Al_2O_3 nanofluid. An experimental rig was locally fabricated and set up to examine MHD mixed convection in an inclined elliptic enclosure subjected to continuous heat flux at the center of the test-section of 0.4 m with the aid of a surface heater, and the top air was cooled, while the 0.3 m on either side of the geometry were insulated using fiberglass of 1.5 cm thickness. The effects of nanoparticle volume fractions and inclination angles on the thermal field were examined and discussed under laminar flow conditions. The results showed that the magnetic field effect on nanoparticle volume concentrations deteriorated with fluid flow strength (velocity profiles). At 0° inclination angle, 28% heat transfer enhancement was achieved, while 30° inclination showed 24 % augmentation, and 60° inclination angle presented approximately 23% enhancement. Additionally, the rate of heat transfer for φ at 4.5% (0.045) nanoparticle volume fraction was found to be almost 10% higher than that of the base fluid (distilled water), φ at 0%. Close observation revealed that, in all cases, T_{wall} values were slightly higher than T_{fluild} and both increased with inclination angle and nanoparticle volume fraction. The percentage difference for Re at 400 mm, 600 mm, and 800 mm values along the axial direction with respect to the rate of heat transfer was not significant for angles of inclinations 0°, 30° and 60°.

1. Introduction

Diverse convective heat transfer and fluid-flow phenomena in irregularly shaped geometries are significant in engineering and technology owing to their widespread applications, including the cooling of microelectronic equipment, heat exchangers, and solar collectors [1]. Unrestricted and forced convective flows as well as heat transfer in enclosures have been intensely studied, originally in astrophysics, as in solar structure and geophysics, as in planetary magnetism, MHD pumps, MHD generators, nuclear reactors, electromagnetic casting, metallurgical processing, stability of convective flows, and several others [2-9]. One of the unique aspects of MHD is that the gas is not constrained by a wall and is therefore subject to unsteadiness and waves, yet it is free surface. A closely related application is in MHD accelerators, which are used to inject plasma into fusion devices or to produce higher-energy wind tunnels for achieving hypersonic flight. Other relevant applications of MHD include electromagnetic with fluid conductors, several storage devices, energy conversion appliances, and control mechanisms in material manufacturing industries [8-10]. The study of magnetohydrodynamics (MHD) flow and heat transfer in electrically conducting fluids is common in electrical power generation, astrophysical flows, and solar power technology [11]. Also, further engineering and industrial circumstances where mixed convective heat transfer in the presence of a magnetic field is relevant include cooling of electronic devices, furnace design, flow and heat

transfer in obstructed cavities such as micro-electronic devices, flat plate condenser in refrigeration systems, production of steel and aluminum, high- performance super-alloys or crystal among others [12]. Again, it is imperative to note that the exceptional performance of any electronic equipment is predicted by their operating temperature. Continuous cooling is highly needed to keep electronic devices within the expected temperature range. Increasing heat transfer rate, compactness and reliable operation are the problems confronting electronic device experts and researchers. These problems have called the attention of researchers and electronic experts to intensify their efforts on studying mixed convective heat transfer since it is the source of air cooling system used [11-13]. Nanofluids are dilute liquid suspension of nanoparticles or mixtures of base fluid with a very diminutive amount of solid metallic oxides with at least one critical dimension smaller than 100 nm which was originally used by Choi [14]. In recent times, more attention is paid to nanotechnology because of its improved properties associated with heat transfer. Nanofluid is useful in buildings, heating, heat exchangers, power plants, automobile cooling applications, cooling of electronic devices, cooling of transformer coil, transportation industry, microchips and solar absorption to mention a few [15].

The roles of nanofluids are numerous considering the h eat exchanger devices for different engineering and industrial applications [16]. Base fluids, such as water plays a significant role in heat transfer enhancement in some industrial applications, such as in cooling of microelectronics, transportation systems and manufacturing processes. The cooling efficiency needed for these applications is often not accomplished with base fluid only, the reason for the usage of Al_2O_3-water based nanofluid considered in this study. And if cooling efficiency is on the increase, there would be increase in life span of the equipment. In the same vein, several industrial applications where loads are essential but have limited space, require tubular heat exchangers are required to be incorporated for the cooling of the electronic equipment. In such cases, a compact, effective, efficient and durable heat exchanger would be needed for the numerous industrial applications [17,18]. Majid et al. [19] considered a fundamental study on development of MHD generator on wave energy harvesting experimentally. Effect of intensity of NaCl solution (sea water), flow rate, magnetic strength and magnetic positioning to the power generated were studied. They concluded that each factor aforementioned showed an important effect in relation to the power generated and play a prominent role on the developed MHD generator to harvest energy as a unique approach to meet the demand for energy. Sharme et al. [20] investigated MHD generator for power generator in huge size using heat combustion. They concluded that the latest development in the MHD technologies have improved from 35% to around 70%, thereby making MHD system much closer to the conventional method. Goel et al. [21] established that the thermo-dynamic conversion system (turbine) has huge losses. And, the demand for energy supply for man use is ever increasing, so from the effectiveness and dependability standpoint, MHD generator is promising for meeting the demand for future energy consumption.

Putral et al. [22] presented free convective flow using CuO-H_2O and Al_2O_3-H_2O combinations in a horizontally positioned cylinder subjected to different thermal boundary conditions. They concluded that convective heat transfer coefficient (h) declined with the application of nanofluids. Wen and Ding [23] reported experimental study on free convection using TiO_2–H_2O combination between two parallel discs. The results indicated that convective heat transfer coefficient (h) decreased with nanofluid mixtures related to water and supported their results with mechanisms to elucidate this behavior. Heris et al. [24] presented experimentally the convective heat transfer coefficient of Al_2O_3-H_2O and CuO-H_2O nanofluids for laminar flow condition in an annular tube subjected to continuous wall temperature. They concluded that the convective heat transfer coefficient elevated with elevating Peclet number and elevating nanoparticle volume concentrations. The enhancement was more with Aluminium water mixture than copper-water combination. Fotukian and Esfahany [25] investigated experimentally convective heat transfer in turbulent condition within a tube using Al_2O_3-H_2O nanofluid. The researchers concluded that there was 48 % increase in heat transfer coefficient compared to pure water for 0.054 % volume concentration at Re=10,000. Also, the study established that increasing the nanoparticle volume fraction did not show significant effect on heat transfer enhancement. Again, the researchers confirmed as well that pressure drop of nanofluid elevated with increasing nanoparticle volume fraction. Bahremand et al. [26] experimentally investigated turbulent nanofluid flow in helically coiled tubes subjected to constant wall heat flux using Eulerian-langrangian technique. The researchers concluded that nanofluid of higher nanoparticle volume fraction enhanced greater heat transfer coefficient and pressure drop.

Gaffar [27] investigated experimentally mixed convective flow in incline circular tube with Al_2O_3-water and hybrid nanofluid. He concluded that experiment 1 (i.e thermally developing laminar mixed convection flow of water and water/ Al_2O_3 mixture in an inclined copper tube subjected to uniform heat flux) showed that the application of nanoparticle volume concentration from (0-4%) resulted in a deteriorating rate of heat transfer for horizontal orientation but the rate of heat transfer was found to be almost constant for vertical inclination both subjected to the same conditions. Also, experiment 2 presented that Nusselt number elevated with Al_2O_3-Cu/ hybrid nanoparticle application (10.95%) than pure water. Also, convective heat transfer coefficient (h) augmented with increasing Reynold number (Re=1730), the result showed optimum heat transfer augmentation of 13.56%. Mansour et al. [28] experimentally studied mixed convection in a circular tube filled with water- Al_2O_3 nanofluid with uniform heat flux. The study established that:

- Elevating nanoparticle volume concentration (0-4 %) retarded the rate of heat transfer for horizontal orientation. But the rate of heat transfer was found to be constant for the vertical inclination orientation both subjected to the same condition
- There is discrepancy between the experimental, analytical and numerical data in terms of heat transfer augmentation under buoyant forces with respect to the usage of single

phase and homogenous fluid model for nanofluid with free convection influence.

Amin [29] investigated experimental and numerical analyses of laminar forced convection in a triangular enclosure filled with TiO_2-water nanofluid. He concluded that the use of nanofluid in the study retarded the wall temperature but augmented Nusselt number (Nu) by 5% with 0.6% and 12% nanofluid volume concentrations. Also, it was revealed from the results that increasing the values of Re number augmented the rate of heat transfer. Thamer et al. [30] experimentally studied thermally developing mixed convection in a horizontal equilateral triangular channel. They concluded that both the temperature ratio and local Nusselt number increased with increased flowrate. Based on the reviewed literatures and to the best of authors' knowledge, there is no experimental article reported on elliptic geometry subjected to constant heat flux with effects of inclination angles most especially the one that concerns MHD systems in which nanofluid is being used as working fluid. This identified gap motivated the authors to investigate MHD mixed convective fluid flow in an inclined elliptic configuration with constant heat flux using Al_2O_3-water nanofluid for different nanoparticle volume fractions (0.0, 0.025, 0.035 and 0.045) which has not been previously considered in published literature.

2. Material and methods

Figure 1 illustrates the design of experimental test rig.

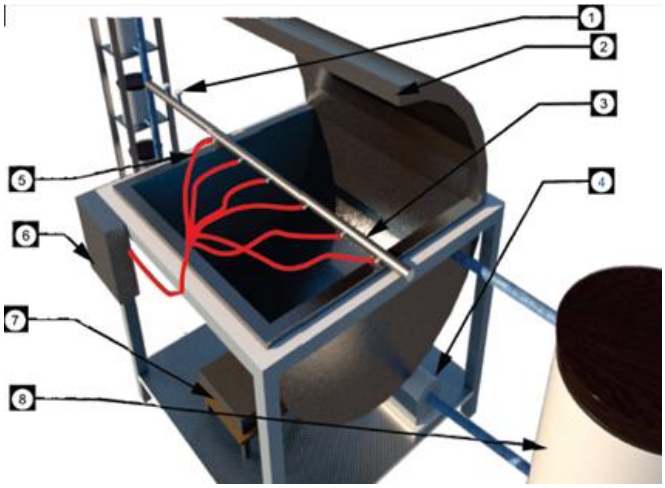

S/NO	DENOTATION
1	PRESSURE GAUGE
2	ELLIPTIC BODY
3	18 MM COPPER TUBE
4	0.5 HP CENTRIFUGAL PUMP
5	K-TYPE THERMOCOUPLE
6	DATA-LOGGER
7	SURFACE HEATER
8	RESERVOIR

Figure 1. The design of experimental test rig

Several studies (numerical and experimental) have estimated the nanoparticle properties based on the base fluid and nanoparticle. The conventional model obtained for a two-phase mixture with numerous experimental results are presented by researchers Wang et al. [31]. For this study, the under- listed equations were employed or adopted for the thermo-physical properties.

Density of nanofluid is computed as follows:

$$\rho_{nf} = (1 - \varphi)(\rho_{bf} + \varphi\rho_p) \quad (1)$$

Specific heat capacity of nanofluid is given as:

$$(\rho C_p)_{nf} = (1 - \varphi)(\rho C_p)_{bf} + \varphi(\rho C_p)_p \quad (2)$$

The thermal expansion coefficient of nanofluid is computed as follow:

$$(\rho_\beta)_{nf} = (1 - \varphi)(\rho_\beta)_{bf} + \varphi(\rho_\beta)_p \quad (3)$$

The Dynamic viscosity of nanofluid is given as:

$$\mu_{nf} = \mu_{bf}(123\varphi^2 - 7.3\varphi + 1) \quad (4)$$

The Thermal conductivity of nanofluid is computed as follows:

$$\frac{K_{nf}}{K_{bf}} = \left[\frac{K_p + 2K_{bf} - 7.3\varphi(K_{bf} - K_p)}{K_p + 2K_{bf} - \varphi(K_{bf} - K_p)}\right] \quad (5)$$

The Thermal diffusivity of the nanofluild is given as,

$$\alpha_{nf} = \frac{K_{nf}}{(\rho c_p)_{nf}} \quad (6)$$

The Electrical conductivity of nanofluid is given as:

$$\sigma_{nf} = (1 - \varphi)\sigma_{bf} + \varphi_p \quad (7)$$

Where bf is basefluid, nf is nanofluid and P is solid particles. The appropriate thermo-physical properties used in this study are presented in Table 1. Also, the dimensionless governing equation employed in this study are presented in equation (8 - 10) [28].

$$\mathrm{Re} = \frac{\rho VD}{\mu} \quad (8)$$

$$\mathrm{Pr} = C_p\,\mu/k \quad (9)$$

$$\mathrm{Gr} = \rho^2 g\beta q_{net} D^4/k\mu^2 \quad (10)$$

Where v is the fluid axial velocity at the enclosure entrance and q_{net} is the difference in heat flux. The experimental convective heat transfer coefficient (h(z)) and the rate of heat transfer (Nu) are computed using equations (11) and (12) correspondingly.

$$h(z) = \frac{q''net}{T_w(Z) - T_f(Z)} = \frac{q_{Total\ supplied} - q_{loss\ at\ the\ exit}}{T_w(Z) - T_f(Z)} \quad (11)$$

$$\mathrm{Nu}\ (z) = \frac{h(z)D}{K} \quad (12)$$

Where D is the diameter of the copper tube used (18mm).

Table 1. Thermo-physical properties of the base fluid (distill-water) and solid nanoparticle

Properties	Base fluid (water)	Nanoparticle (Al_2O_3)
Cp (JKg.k)	4179	773
K(W/m.k)	0.612	35
ρ (Kg/m^3)	998.0	3980
μ (Kgm^{-1}s^{-1})	0.001003	-
N	-	13
β	2.1 x 10^{-4}	0.85 x 10^{-5}

Where Cp is specific heat capacity (J/KgK), K is thermal conductivity (W/mK), ρ is density (Kg/m^3), μ is dynamic viscosity (Kgm^{-1}s^{-1}), n is nanoparticle size (nm).

2.1 Procedures in nanofluid preparation

In this experimental study, two-phase approach was adopted because of its stability and in-expensiveness. The dry nanoparticles (Al_2O_3) were analyzed using Scanning Electron Microscope (SEM). In order to homogenize or mix the nanoparticle and basefluid (distil water) uniformly, take-away pack was first of all used to allow the sonicator vibrator force itself through the mixture very well. MH 2800 Branson type sonicator was used. Each nanoparticle volume fractdistilleds prepared with 2 liters of distil water. Also, from equation 13, mass of the water was calculated. The masses of nanoparticles used in this study were 0.3 g, 0.5 g, 0.7 g and 0.9g and corresponding nanoparticle volume fraction (φ_V) calculated from equation 15 were 0.015, 0.025, 0.035 and 0.045. And since the densities of both water and nanoparticle are known to be 998 kg/m^3 and 3980 kg/m^3 individually. The unknown parameters such as nanoparticle mass and volume fractions were determined from the formulars expressed in Equations (13-15):
The Density of nanofluid is computed as:

$$\text{Density}=\frac{mass}{volume} \tag{13}$$

$$\text{That is } \rho = \frac{m}{v} \tag{14}$$

$$\varphi_{V=}\frac{V_p}{V_{p+}V_o}=\frac{\frac{m\varphi_m}{\rho_p}}{\frac{m\varphi_m}{\rho_p}+\frac{m(1-\varphi_m}{\rho_o}}=\frac{\varphi_m}{\rho_{p(\frac{\varphi_m}{\rho_p}+\frac{1-\varphi_m}{\rho_o})}} \tag{15}$$

Where φ_v and φ_m are respectively volume and mass fraction, ρ_p and ρ_o represents densities of solid particle and base fluid and V_P and V_o stands for volume of solid particle and volume of base fluid (Hao et al. [32]).

2.2 Experimental procedures and flow cycle

The elliptic enclosure was cooled at the top with fan, subjected to continuous heat flux below while the extreme ends were insulated. The fluid (nanofluid) flows from the lower-level tank with the aid of pump (forced convective mechanism) to the upper reservoir having 5-liter capacity for the determination of the appropriate flow rate using a standard stopwatch and measured in seconds. The control valve regulated the fluid flow and transferred to the test-section via the copper tube drilled at 200 mm interval to each other. Thermocouples K-Types with sensors were attached to the drilled points along axial direction The pressure drops were measured by the pressure gauges attached to the enclosure. Two magnets were placed in between the gauges to check for the influence of magnetic field on fluid flow pattern. Surface heater was first switched on for 30 minutes to heat up uniformly the base fluid introduced to the lower part of the enclosure, a portion covering 0.4 m and placed between the insulated parts of 0.3 m along the axial direction. The first thermocouple at the entrance of the test-section recorded the incoming fluid's temperature, the one placed at the exit recorded the temperature of the fluid leaving the enclosure while the remaining four measured the temperatures of the nanofluid, and the wall at the insulated region. A computer attached to the data logger (Ardino type) recorded and stored data (temperature behavior).

3. Results and discussions

Figure 2 presents the effect of nanoparticle volume fractions (ω = 0, 0.015, 0.025, 0.035 and 0.045) on mean axial velocity in axial direction for power supply, P =1.276 -1.41 kW, volumetric flow rates, Q =0.0001923076, 0.0001941748 and 0.0001960784 m^3/s. It was shown from Figure 2 that when magnetic field was not included, the fluid flow velocity for φ=0 has the highest mean axial velocity. The reason is due to the buoyancy force dominating the fluid flow in the axial direction of elliptic geometry. But on the other hand, when the nanoparticle volume fractions varied, the velocities of the fluid flow started reducing. Figures 3-8 present the effect of nanoparticle volume fractions on inclination angles, bulk wall and fluid temperatures along axial direction at a power supply, P = 1.3 kW, volumetric flow rate, Q = 0.0001960784 m^3/s. From the Figures, the bulk wall and fluid temperatures increased by elevating nanoparticle volume fractions. And this is in support of the energy balance equation; $T_f(z) = T_{in} + \frac{q''net\pi DL}{m\,Cp}$ z , where T_{in}, m, Cp represents the inlet fluid temperature of the test section, the mass flow rate, the fluid heat capacity while q"net is the difference between total heat supplied and heat loss, D is the diameter of the tube,L is length and z is axial direction.

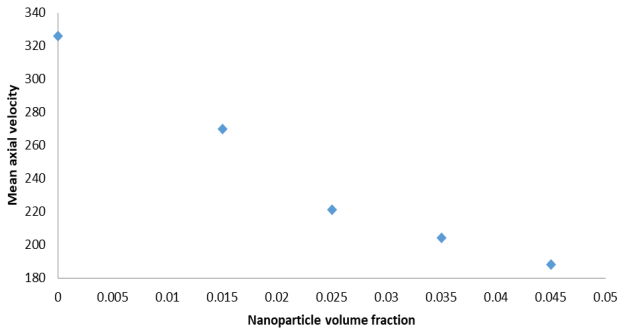

Figure 2. Effect of nanoparticle volume fractions (ω = 0, 0.015, 0.025, 0.035 and 0.045) on mean axial velocity in axial direction

It was clearly shown from the Figures also that both the bulk wall and the fluid temperatures increased with augmenting angles of inclination (0^0, 30^0 and 60^0) as well. In reality, the nanoparticle volume fraction and angles of inclination play a prominent role on both the bulk wall (Figures 3-5) and fluid temperatures as shown in Figures 6-8. Moreover, as indicated in Table 2 and Table 3 derived from Equations (1-7), the heat capacity, Cp for ω = 4.5 % was about 4 % lower than that of the base fluid (water), ω = 0 %. But the variation between the bulk temperature of the outlet and inlet of the test section was found to be 9.87 %.

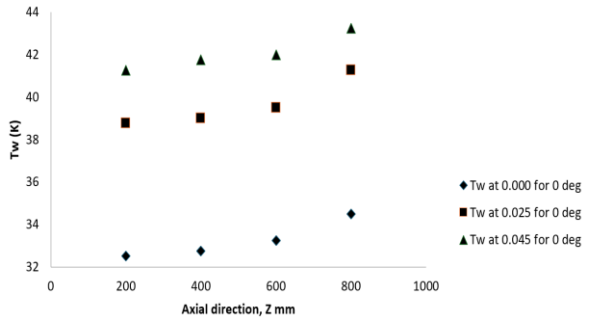

Figure 3. Effect of nanoparticle volume fractions and inclination angle at 0 degree on axial development of temperature (T_w) for a power supply, P = 1.3 kW, volumetric flow rate, Q = 0.0001960784 m^3/s.

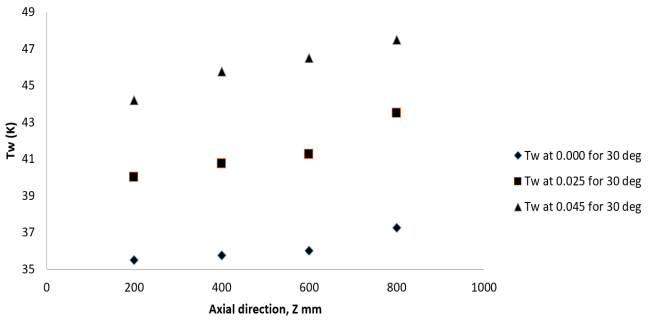

Figure 4. Effect of nanoparticle volume fraction and inclination angle at 30 degree on axial development of temperature (T_w) for a power supply, P = 1.41 kW, volumetric flow rate, Q = 0.0001960784 m^3/s.

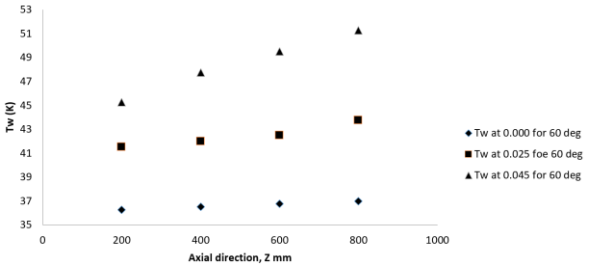

Figure 5. Effect of nanoparticle volume fractions and inclination angle at 60 degree on axial development of temperature (T_w) for a power supply, P = 1.41 kW, volumetric flow rate, Q = 0.0001960784 m^3/s.

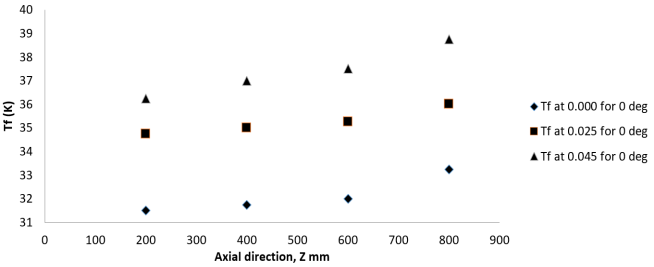

Figure 6. Effect of nanoparticle volume fractions and inclination angle at 0 degree on axial development of temperature (T_f) for a power supply, P = 1.28 kW, volumetric flow rate, Q = 0.0001941747 m^3/s.

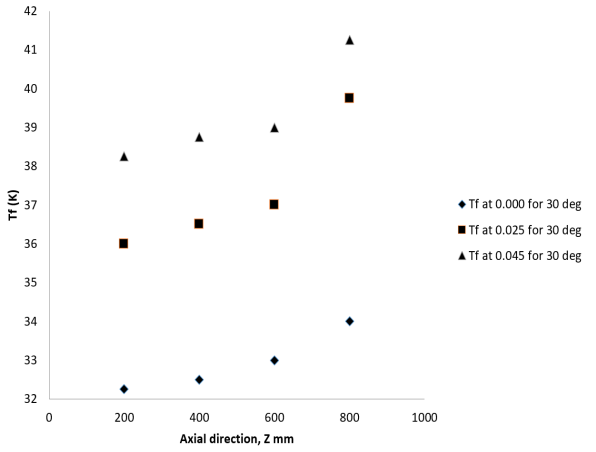

Figure 7. Effect of nanoparticle volume fractions and inclination angle at 30 degree on axial development of temperature (T_f) for a power supply, P = 1.27 kW, volumetric flow rate, Q = 0.0001941747 m^3/s.

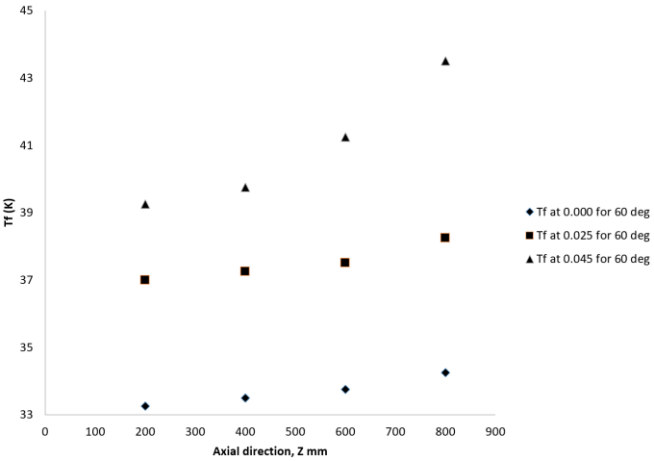

Figure 8. Effect of nanoparticle volume fractions and inclination angle at 60 degree on axial development of temperature (T_f) for a power supply, P = 1.27 kW, volumetric flow rate, Q = 0.0001960784 m^3/s.

Again, the figures also revealed that the distinction between the wall and fluid temperatures (T_w - T_f) augmented slightly and consistently with both the increasing nanoparticle volume fraction and inclination angles but the values for the T_w are slightly higher than the T_f (Mansour et al. [28]). Deductions drawn from Table 2 and 3 for nanoparticle volume fraction at ω = 0.00 and 0.045 showed that the elevating thermal conductivity (K) augmented by 13.37 %, the expansion coefficient (β) deteriorated by 4.48 % and the dynamic viscosity (μ) gave 48.37 %. Equations (1-7) model were used to generate the values of K_{nf}, μ, ρ in Table 4. The percentage change in thermal conductivity (K) was calculated from the relationship between nanoparticles volume fraction (ω) and thermal conductivity K_{nf} respectively. Table 4 presents the variation of percentage increase of thermal conductivity, thermophysical properties with the nanoparticle volume fraction.

Figures 9-11 depict the effect of nanoparticle volume fractions and inclination angles on axial development of heat transfer coefficient (h) for P=1.27-1.41 kW, Q =0.0001923076- 0.0001960784 m^3/s, angles of inclination (0^0, 30^0 and 60^0) and nanoparticle volume fractions (ω = 0.00, 0.025 and 0.045). The Figures showed that for the same volumetric flow rate and fixed power supply, the inclination angles and nanoparticle volume fractions resulted in deteriorating convective heat transfer coefficient (h).

Table 2. Thermophysical properties of various phases for ω = 0.00 (base fluid)

Property	Fluid phase (water)	Solid phase (Aluminium oxide particles)
ρ_{bf} (kg/m^3)	998.0	ρ_p = 3980
Cp_{bf} (Jkg/k)	4179	$(Cp)_p$ = 773
β_{bf} (K^{-1})	2.1 x 10^{-4}	β_p = 0.85 x 10^{-5}
μ_{bf}	0.001003	-
K_{bf} (w/mk)	0.612	Kp = 35
N	-	13

Table 3. Thermophysical properties for ω =0.045 (nanoparticle volume fraction)

Property	Nanofluid phase
ρ_{nf}	1132.2
$(\rho Cp)_{nf}$	4025.73
$(\rho\beta)_{nf}$	2.01 x 10^{-4}
μ_{nf}	6.76 x 10^{-4}
K_{nf}	0.693845

Table 4. Variation of thermophysical properties with the nanoparticle volume fractions

ω	Thermal conductivity K_{nf} (W/mK)	μ (Ns/m)	Density ρ (kg/m^3)	% change in thermal conductivity (K)
0	0.612	0.001003	998.0	-
0.015	0.6386	0.000921	1042.7	4.35%
0.025	0.656574	0.000898	1072.6	7.28%
0.035	0.675099	0.000897	1102.4	10.31%
0.045	0.693845	0.000676	1132.2	13.37%

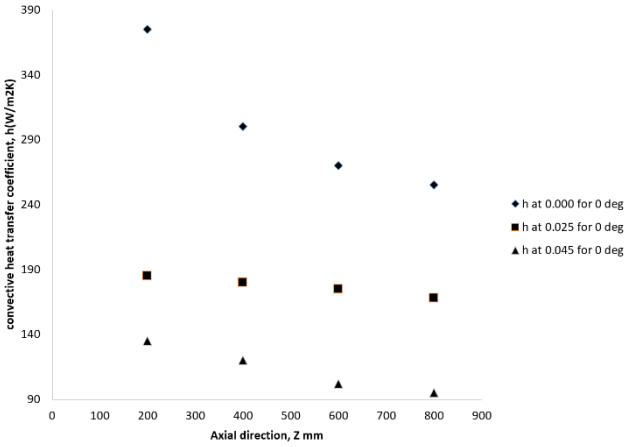

Figure 9. Effect of nanoparticle volume fraction and inclination angle at 0 degree on axial development of heat transfer coefficient (h) for P =1.3 kW, Q = 0.0001960784 m^3/s.

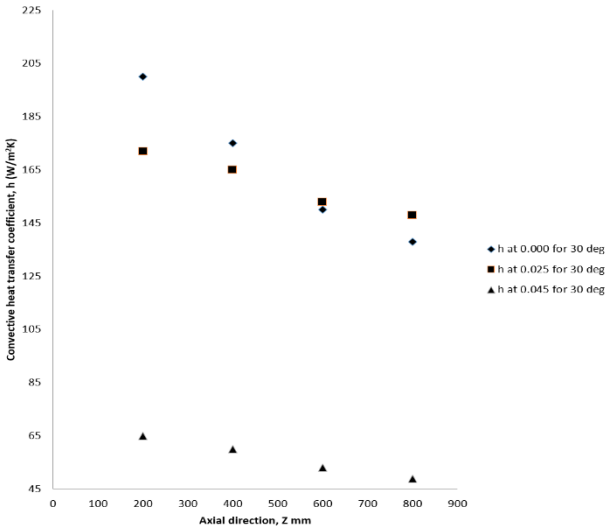

Figure 10. Effect of nanoparticle volume fraction and inclination angle at 30 degree on axial development of heat transfer coefficient (h) for P = 1.3 kW, Q = 0.0001960784 m^3/s.

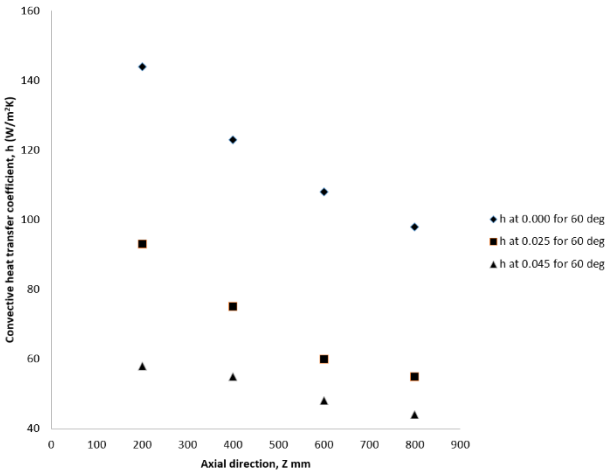

Figure 11. Effect of nanoparticle volume fraction and inclination angle at 60 degree on axial development of heat transfer coefficient (h) for P = 1.3 kW, Q = 0.0001960784 m^3/s.

The Figures clearly showed that the values were higher in 0 degree inclination (horizontal) than 30 degree (inclined) while the least was recorded for 60 degree inclination but all showed same trend. The results revealed that heat transfer characteristics of the nanofluid are not determined principally by the effective thermal conductivity (K) alone, different thermophysical properties such as density, thermal expansion coefficient, and heat capacity can play prominent roles or alter the heat transfer behavior of nanofluid for both free and forced convection (Gaffar [27], Mansour et al. [28]).

Figures 12-14 show the variation of Nusselt number on inclination angles and nanoparticle volume fractions in axial direction for a fixed power supply, P = 1.27 kW and Q = 0.0001960784 m^3/s. The Figures indicated that the Nusselt number decreased with the increasing angles of inclination and elevating nanoparticle volume fractions. Between the angle of inclination 0^0 and 30^0, the Nusselt number deteriorated by 3.29 % while between 30^0 and 60^0 inclination angles, the rate of heat transfer decreased by 10.57 %. Between 0.00 and 0.045 nanoparticle volume fractions, the

rate of heat transfer reduced from 9.73 to 7.34, a relative reduction of almost 24.56 %.

The reason behind this behavior of nanofluid was caused by a very strong secondary flow generated by natural convective motion (buoyancy force) when compared with the base fluid (Mohammad et al. [13]). The characteristic is also in agreement with the published research on experimental investigations of free convective flow motion of nanofluids in various enclosures. The Figures showed that the rate of heat transfer (Nu) is not dependent on the nanoparticle volume fractions (Putra et al. [22], Wen and Ding [23], Gaffar [27], Mansour et al. [28]). Figure 15 presents the effect of Reynold number in the fully developed region for 0^0 inclination angle and nanoparticle volume fractions, power supply P=1.3 -1.41 kW and Q= 0.0001923076 -0.0001960784 m^3/s. From Figure for 0^0 inclination, the rate of heat transfer (Nu) did not vary significantly with Reynold number. The highest percentage difference for Re at 400, 600 and 800 with respect to the rate of heat transfer was 1.17 %. The Figure also revealed that Nusselt number decreased with both the increasing Reynold number and nanoparticle fraction.

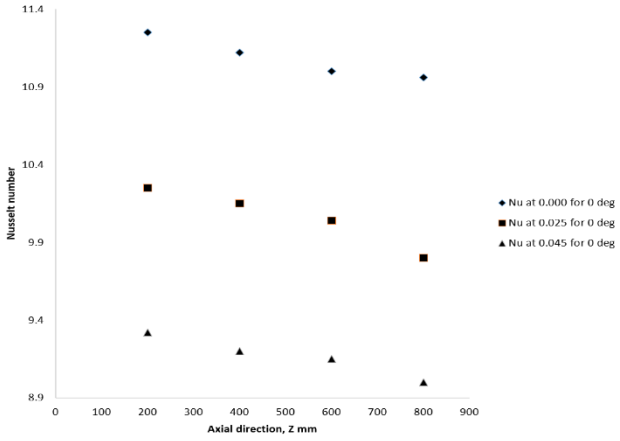

Figure 12. Variation of Nusselt numbers on the inclination angle 0^0 and three particle volume fraction (0.00, 0.025 and 0.045) in axial direction for a fixed power supply, P = 1.3 kW and Q = 0.0001960784 m^3/s.

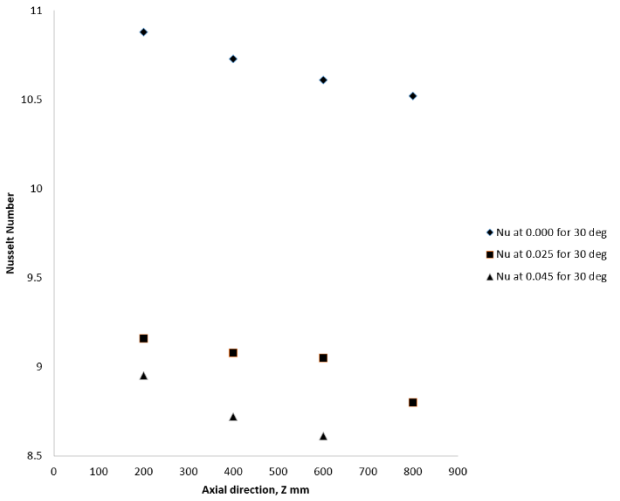

Figure 13. Variation of Nusselt number on the inclination angle 30^0 and three particle volume fraction (0.00, 0.025 and 0.045) in axial direction for a fixed power supply, P =1.27 kW and Q = 0.0001960784 m^3/s.

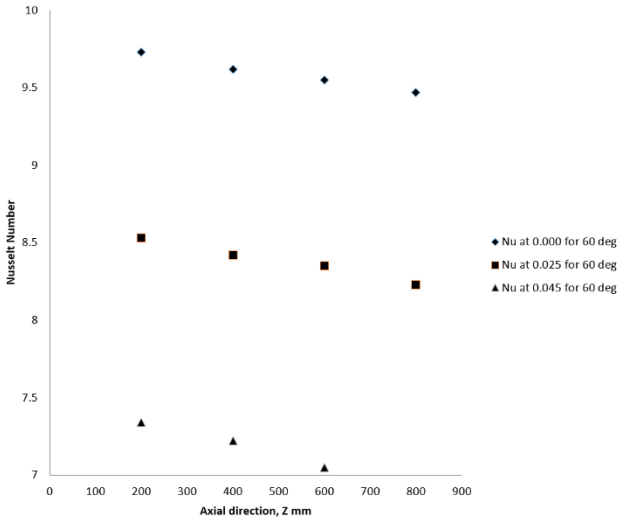

Figure 14. Variation of Nusselt number on the inclination angle 600 and three particle volume fraction (0.00, 0.025 and 0.045) in axial direction for a fixed power supply, P = 1.3 kW and Q = 0.0001960784 m^3/s.

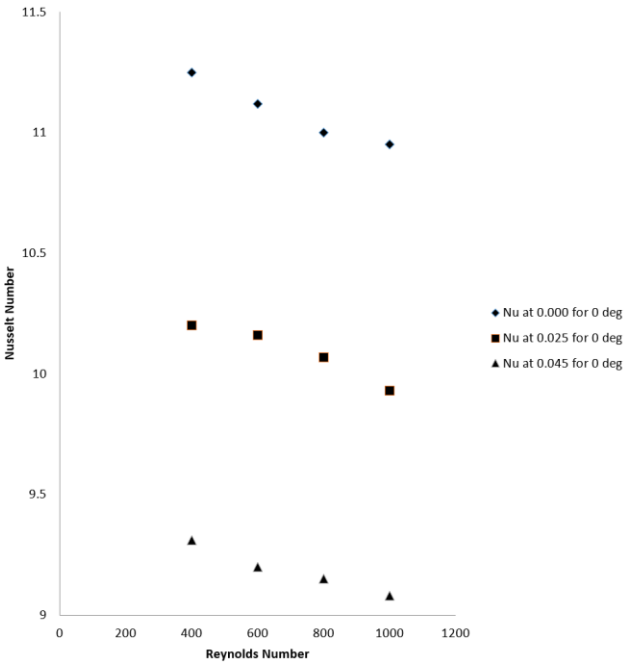

Figure 15. Effect of Reynold number in the fully developed region for 00 inclination angle and various nanoparticle volume concentrations (ω = 0.00, 0.025 and 0.045), power supply P=1.4 kW and Q = 0.0001960784 m^3/s.

Figure 16 presents the effect of Reynold number in the fully developed region for 30^0 inclination angles, different volume fractions, and fixed power supply. For 30^0 inclinations, effect on the Reynold number, the rate of heat transfer followed similar trend to that of 0^0 inclination (not significant). The highest percentage difference between the rate of heat transfer and Reynold number was found to be 1.47 %.

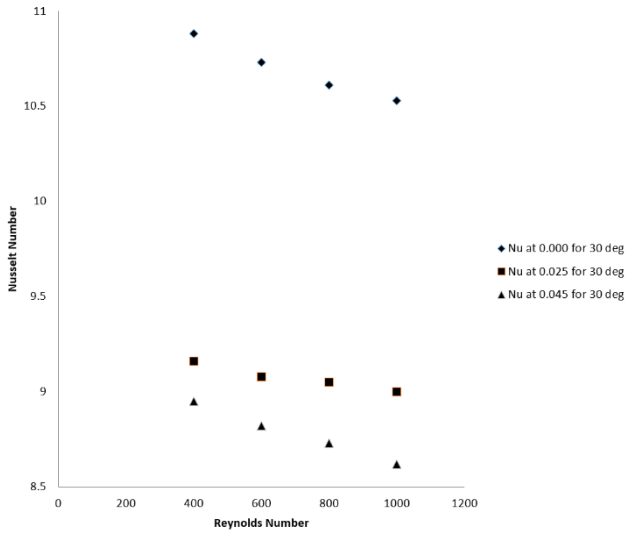

Figure 16. Effect of Reynold number in the fully developed region for 30^0 inclination angle and three nanoparticle volume concentrations (ω = 0.00, 0.025 and 0.045), power supply P=1.3 kW and Q = 0.0001960784 m^3/s.

In the same vein, Figure 17 shows the effect of Reynold number in the fully developed region for 60^0 inclination angle and various nanoparticle volume fraction. The highest percentage difference with respect to the relationship between the Nusselt number and increasing Reynold number was found to be 1.31 %.

Figure 18 shows the effects of Grashof number on 0^0 inclination angle in the fully developed region, different nanoparticle volume fraction, fixed power supply, P = 1.3kw and Q =0.0001923076- 0.0001960784 m^3/s. It was observed that the rate of heat transfer increased with elevating Grashof number. From Figure 18 for 0^0 inclination, the rate of heat transfer elevated from 7.15 for 10^4 values of Grashof number to 9.12 for 10^6 values. It showed an improvement in terms of heat transfer up to 27.55%. For nanoparticle volume fraction at ω = 0.045, the critical examination of Figure 10 indicated that the rate of heat transfer (Nu) deteriorated with increasing nanoparticle volume fraction (ω = 0.0 to ω = 0.045). The reason for the reduction in the rate of heat transfer was due to insignificant buoyancy force (free convention effect) as a result addition of alumina particles in the nanofluid. For ω = 0.025 and ω = 0.045, the rate of heat transfer enhancement reduction was found to be 9.7 % and 20.8 % respectively.

In the same vein, Figure 19 depicts the effect of Grashof number on 30^0 inclination angle in the fully developed region and for the same nanoparticle volume fraction considered. The figure showed similar trend and the rate heat transfer increased from 6.56 to 8.15 for Grashof number 10^4 and 10^6 respectively. It has an enhancement in terms of heat transfer up to 24.23 %.

The reason for this behavior is similar to the explanation given in Figure 18. and when the rate of heat transfer reduction was compared with ω at 0.0 (base fluid) for ω=0.025 and 0.045, they followed similar trend but by 13.32 % and 21.32 % reduction respectively.

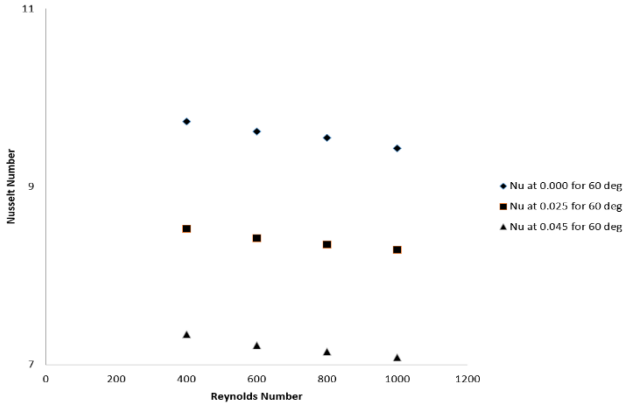

Figure 17. Effect of Reynold number in the fully developed region for 60^0 inclination angle and three nanoparticle volume concentrations (ω = 0.00, 0.025 and 0.045), power supply P=1.3 kW and Q = 0.0001960784 m^3/s.

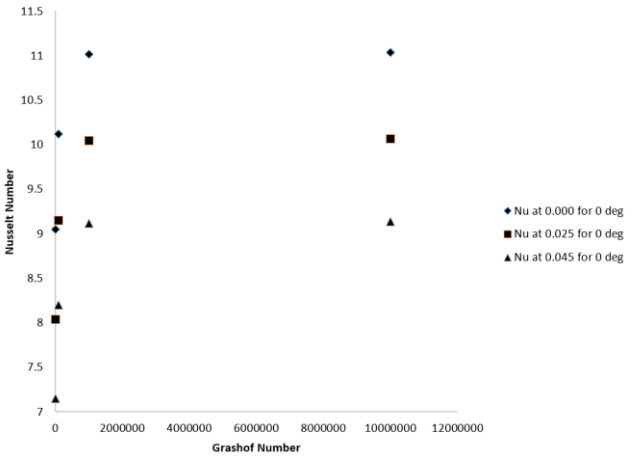

Figure 18. Effects of Grashof number with 0^0 inclination angle in the fully developed region, for the various particle volume fraction (ω = 0.00, 0.025 and 0.045), fixed power supply, P = 1.4 kW and Q = 0.0001960784 m^3/s.

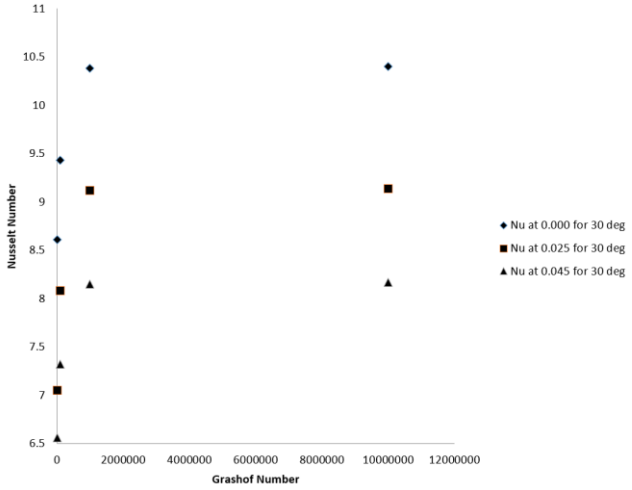

Figure 19. Effects of Grashof number with 30^0 inclination angle in the fully developed region, for the three particle volume fraction (ω =0.00, 0.025 and 0.045), fixed power supply, P = 1.27 kW and Q = 0.0001960784 m^3/s.

Figure 20 shows the effect of Grashof number on 60^0 inclination angle (inclined position) for a fixed power supply P = 1.41 kW, Q = 0.0001923076-0.0001960784 m^3/s and different nanoparticle volume fractions. The figure indicated same trend with 0 ^{0} and 30 ^{0} inclination separately. The Nusselt number increased from 5.20 to 6.40 as Grashof number increased from 10^4 to 10^6. Heat transfer enhancement up to 23.08 % was observed with nanoparticle volume fraction, ω = 0.045. The same reason stated in Figures 18 and 19 accounted for this insignificant buoyancy force effect. Again, when the rate of heat transfer reduction was compared with ω at 0.000 (base fluid) with ω at 0.025 and ω at 0.045, the reduction in terms of the rate of heat transfer were found to be 13.5 % and 27.03 % one-to-one. It can therefore be concluded for Figures 18-20 with respect to the Grashof number between 10^4 to 10^6, the rate of heat transfer (Nu) increased significantly with Grashof number but deteriorated with increasing nanoparticle volume fraction (ω = 0.000, 0.025 and 0.045) and inclination angles (0 ^{0}, 30 ^{0} and 60 ^{0}) but the rate of heat transfer enhancement between angle 30^0 and 60^0 was minimal. Figure 21 and Figure 22 illustrate the validation of experimental results, where Figure 21 shows comparison of results from present investigation (experimental study) on effect of φ and Gr on Nusselt Number for horizontal tube, $\theta = 0^0$ with Mansour et al. [28] and Figure 22 compares the of results from the present study (experimental investigation) on effects of φ and Re on Nusslt Number for horizontal tube, $\theta = 0^0$ with Mansour et al. [28].

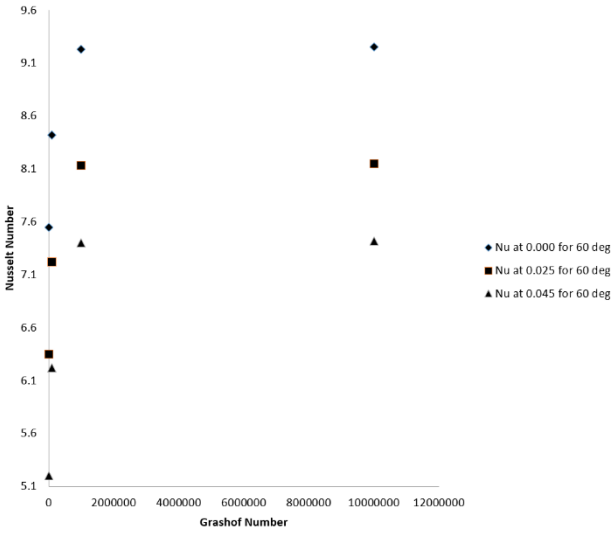

Figure 20. Effects of Grashof number with 60^0 inclination angles in the fully developed region, for the three particle volume fraction (ω = 0.00, 0.025 and 0.045), fixed power supply, P = 1.27-1.3 k\W and Q = 0.0001960784 m^3/s

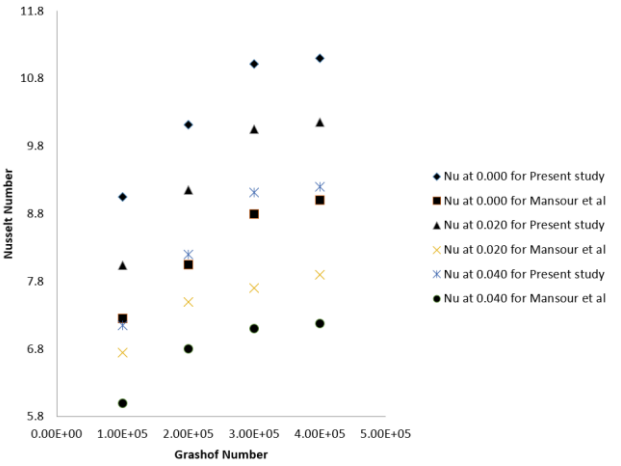

Figure 21. Comparison of results from present investigation (experimental study) on effect of φ and Gr on Nusselt Number for horizontal tube, $\theta = 00$ with Mansour et al. [28]

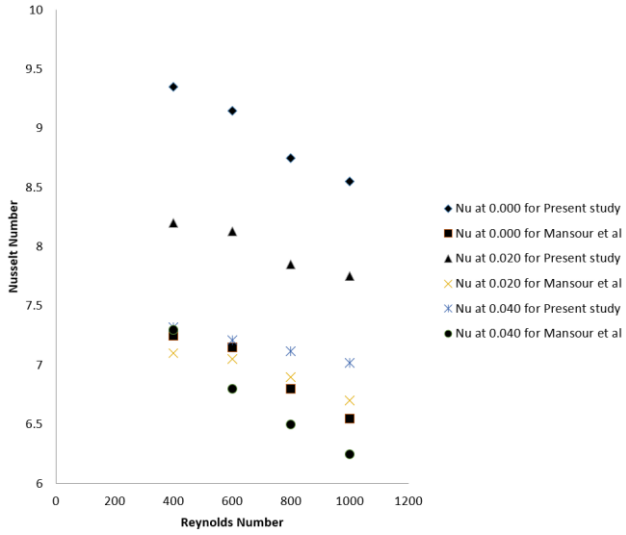

Figure 22. Comparison of results from present study (experimental investigation) on effects of φ and Re on Nusslt Number for horizontal tube, $\theta = 00$ with Mansour et al. [28]

4. Conclusion

Experimental study was carried out to analyze the heat transfer characteristics of Al_2O_3-H_2O nanofluid in an oriented elliptic configuration. The following conclusions were drawn from the investigation:

- The magnetic field effect on increasing nanoparticle volume fraction resulted in deteriorating velocity profile (mean axial velocity).
- The bulk wall (Tw) and fluid temperature (Tf) elevated with increasing nanoparticle volume fraction as well as angles of inclinations. In all cases, Tw increases slightly higher than the Tf.
- The variation of Reynolds number with Nusselt number was not significant for inclination angles 0,30 and 60 degrees
- Heat transfer behavior of the nanofluid is not characterized only by thermal conductivity but other thermophysical properties such as density, heat capacity and thermal expansivity are involved

- At the same fixed power supply and flow rate, the convective heat transfer coefficient (h) deteriorated with increasing inclination angle and nanoparticle volume fraction.
- The rate of heat transfer declined with elevating inclination angles and nanoparticle volume fraction
- Nusselt number elevated with elevating Grashof number but its enhancement reduced with increasing inclination angles and volume fractions.

Ethical issue

The authors are aware of and comply with best practices in publication ethics, specifically concerning authorship (avoidance of guest authorship), dual submission, manipulation of figures, competing interests, and compliance with policies on research ethics. The authors adhere to publication requirements that the submitted work is original and has not been published elsewhere in any language.

Data availability statement

The manuscript contains all the data. However, more data will be available upon request from the corresponding author.

Conflict of interest

The authors declare no potential conflict of interest.

References

[1] Al-Salem K., Ozto, H.R.,Pop,I, Varol, Y. (2012). Effects of moving lid direction on MHD convection in a linearly heated cavity. Int. Journal Heat and Mass Transfer, 55, 1103-1112.

[2] F.O.Hakan, S. Ahmad, A. Eiyad, and, A. Khalid, Mixed convection of MHD flow in nanofluid filled and partially heated wavy walled lid-driven enclosure. Int. Comm in Heat and Mass transfer, (2017) 86:42-51.

[3] M.M. Ali, M.A. Alim, and S.S. Ahmed. MHD Mixed convective flow in a Hexagonal enclosure, precedia engineering, (2017) 194:479-486.

[4] S. Kherroubi,N. Ragul, Y.K. Labsi, A. Benkahia, and A. Boutra. 3-D Numerical study of mixed convection within a ventilated cavity filled with nanofluid under the effect of a magnetic field, MATEC web of conference, (2020), 307:1-6

[5] B. Cakagni, F.Marsil, and M.Paroncini. Natural convective heat transfer in square enclosures heated from below. Applied Thermal Engineering, (2005) 25, 2522-2531.

[6] M.M. Rahman, M.A. Alim, and M.M Sarker. Num. study on the conjugate effect of joule heating and MHD mixed convection in an obstructed lid-driven square cavity. Int. Comm. in Heat and Mass Transfer, (2010) 37, 524-534.

[7] B.Mounir, and B.D.Amma. Entropy generation study of MHD thermoslutal convetion in a square cavity for different Prandtl number. Int. J. of Mechanic Application, (2011),2,22-29.

[8] N. Morley, S.,Smolentser, and M. Abdan. MHD and Thermal issue on the SICF/SIC flow channel. Insent, Fusion Science and Technology, (2006) 50, 107-119.

[9] S. Aberkane, M. Ihdere, M. Moderas, and A. Ghezal. Effect of an axial magnetic field on the heat and mass transfer in rotating annulus. Int. Journal. of Physical Science, (2014) 9, 368-379

[10] E.S. Ahmed, A.K. Hussein, H.A. Mohammad, I.K. Adegun, X. Zhang, L. Kolsi,. A. Hasanpow, and S. Sivasankaran. Viscous dissipation and radiation effects on MHD natural convection in a square enclosure filled with a porous medium. Nuclear Engineering and Design (2014), 266, 34-42.

[11] M. Hasanuzzaman, F.O. Hakan, M. M., Raham, N.A. Rahim, R.,Saidur, and Y. Varol. agnetohydrodynamics natural convection in trapezoidal cavities. Int. Comm Heat Mass Transfer, (2012) 31,606-612.

[12] M. Sheikholeslami, M. Gorgi-Bandpy, I. Pop, and S. Soleimami. Numerical study of natural convection between a circular enclosure and a sinusoidal cylinder using control volume base finite element method. Int. Journal of Thermal Science, (2013), 72, 147-158

[13] E.S. Ahmed, A. K., Hussein., H.A. Mohammad, I.K. Adegun, X. Zhang, L. Kolsi, A. Hasanpow, and S. Sivasankaran. Viscous dissipation and radiation effects on MHD natural convection in a square enclosure filled with a porous medium. Nuclear Engineering and Design, (2014),266, 34-42

[14] U .S. Choi. Enhancing thermal conductivity of fluid with nanoparticles. Development and applications of non-newtonian flows. ASME, N/York, FED, (1995), 66, 99-105.

[15] D.A. Emad, K.R.,Hayder, M.J., Hussein, Y.A.,Saba,O.W.Salwan, K.H.Hameed, and H.A.Farooq. MHD influence on mixed convection of annulous circular enclosure filled with Cu-water nanofluid, (2020), https://doi.org/10.1016/j.heliyon. 2020.e03773.

[16] J. Ali ,I. Chamkha, S. Fatih and F.O. Hakan. Effects of a Rotating Cone on the Mixed Convection in a Double Lid-Driven 3D Porous Trapezoidal Nanofluid Filled Cavity under the Impact of Magnetic Field. International Journal of Artificial Intelligence and Mechatronics. (2020),3, 3, 2320 – 5121

[17] D. Ruchika, R. Puneet, and K. Lokendra . MHD mixed convection over an inclined cylinder subjected to velocity and thermal slip effect. Powder Technology, (2016). 288, 140 – 150.

[18] Sakalis,V.D.,Hatzkonstaninoi,P.M.,Kafousias,N. (2002).Thermally developing flow in elliptic ducts with axially variable wall temperature distribution. International Journal of Meat and mass Transfer,45,25-35

[19] M. F. Majid, .M. A, Al-Hakim, M, Sabri, and K. Shahril. Fundamental studies on development of MHD generator implement on wave energy harvesting. Material science and engineering,(2016), 114-1-9.

[20] S. Sharma. and S. Gambhir. MHD power generation Technique. Int. Journal of computing and corporate research 5(5), (2016)1-11

[21] P. Goel and A. Shukle . MHD power generation. Int. Advanced Research of science and engineering Technology (IARJSET) 2(1),(2015),105-107.

[22] N.Putra, W.. Roetzal, S. K.Das.Natural convection of nanofluid heat and mass transfer,39, (2003),775-784.

[23] D.Wen, Y.Ding. Natural convection convection heat transfer of suspension of titanium dioxide nanofluid. IEEE, trans nanotechnology,5, (2006),220-222.
[24] S.Z. Heris,S.G.Etermad,M.N.Esfahany. Experimental investigation of oxide nanofluid laminar flow convective heat transfer coefficient.Int.comm Heat and mass transfer,33, (2006),529-535
[25] S.M.Fotukian and M.N.Esfahany. Experimental investigation of turbulent convective heat transfer of dilute Al2O3/water nanofluid inside a circular tube.Int.J.of Heat and Fluid flow,31,(2010),606-612.
[26] H. Bahremand, A.Abbassi,M.Saffar-Awal. Experimental and numerical investigation of turbulent nanofluid flow in helically coiled tubes under constant wall heat flux using Eularian-langragian approach.269 (2015),93-100
[27] G.M. Gaffar. Experimental study of mixed convection with Al2O3-water and hybrid nanofluid in oriented copper tube for laminar flow. Int. J. of Scientific & Tech research, (2013), 2, 195 – 202
[28] R.B. Mansour, N. Gelami, and C.T. Nguyen. Experimental investigation of mixed convection with water- Al2O3 nanofluid in inclined tube with uniform wall heat flux. Int. J. of Thermal Science, (2011), 50, 403 – 410
[29] J. Amin. Numerical and experimental study of laminar forced convection heat transfer of TiO2-water nanofluid in triangular duct. Int. Journal of Artificial Intelligence and Mechatronics, (2014) 3(3), 107-111
[30] K.S. Thamer, R.J. Raaid, and S.M. Maner. Thermally developing mixed convection in a horizontally equilateral triangular channel, IJRRAS, (2013),16(1,),157-167
[31] X. Wang, X. Xu, and S. U.S. Choi. Thermal conductivity of nanoparticles fluid mixture. Journal of Thermophysics and Heat Transfer,(1999) 13(4), 474-480.
[32] P. Hao, D. Guoliang, H. Haitao. .Influence of refrigerant-based nanofluid composition and heating condition on the migration of nanoparticles. Int .J.of Refrigeration, 34, (2011),1823-1832

This article is an open-access article distributed under the terms and conditions of the Creative Commons Attribution (CC BY) license (https://creativecommons.org/licenses/by/4.0/).